Journal of
Mechanics of
Materials and Structures

OPTIMIZATION OF STIFFENED PANELS CONSIDERING GEOMETRIC NONLINEARITY

Peyman Khosravi, Ramin Sedaghati and Rajamohan Ganesan

Volume 2, Nº 7 September 2007

mathematical sciences publishers

JOURNAL OF MECHANICS OF MATERIALS AND STRUCTURES
Vol. 2, No. 7, 2007

OPTIMIZATION OF STIFFENED PANELS CONSIDERING GEOMETRIC NONLINEARITY

PEYMAN KHOSRAVI, RAMIN SEDAGHATI AND RAJAMOHAN GANESAN

In this study, an optimality criterion is presented for thickness optimization of plate structures with geometric nonlinearity. The optimization problem considers the thickness of each element of the finite element mesh as a design variable and aims to maximize the load-carrying capacity of the structure subject to constant total volume. The result of the thickness optimization of a nonstiffened panel is then used for locating the potential places to add the stiffeners. It is shown that the load-carrying capacity of the original panel may be improved significantly while having the same volume of material. Application of the method is illustrated by numerical examples.

1. Introduction

Structural optimization can be used to improve a design by changing the geometrical properties of the structure, considering a set of design constraints. In structural optimization, the thickness, shape, or topology of the structure is iteratively changed until an optimal design is achieved [Bendsøe 1989; Bendsøe and Mota Soares 1993; Rozvany 1997; Maute et al. 1998; Bendsøe and Sigmund 1999; 2003; Lógó and Ghaemi 2002]. Developing design optimization techniques that efficiently combine the iterative optimization process and iterative analysis of nonlinear structures is a challenging and complex task which has not yet received sufficient attention. Optimization based on nonlinear mathematical programming techniques involves many evaluations of the objective function and constraints at each optimization iteration before a new search direction and step size can be established. This makes the design optimization of nonlinear structures computationally very expensive, as nonlinear analysis by itself is a highly iterative process.

Optimality criterion methods may significantly reduce the time and cost of the optimization process in nonlinear structures. Optimality criteria could be in the form of intuitive criteria, such as fully stressed design (FS), simultaneous failure mode design (SFM), uniform strain energy density design (USED), constant internal force distribution design (CIFD), or mathematically defined equations, such as classical optimality criteria method (COC), dual optimality criteria method (DOC), and general optimality criteria method (GOC) [Lógó 2005].

Gallagher [1973] pointed out that the fully stressed design (FS) criterion is inadequate for minimum weight design of structures. Prager and Taylor [1968] showed that the optimum structure with uniform material properties and linear relation between the stiffness and volume has a uniform energy density distribution. A similar criterion was proposed by Venkayya et al. [1968; 1969] for discretized structures, stating that the average strain energy density is the same for all elements of the optimum structure. Later, Venkayya [1971] developed a more general form for the optimality criteria stating that the ratio of strain energy to strain energy capacity is constant for every member in the optimum structure.

Keywords: thickness optimization, optimality criterion, stiffened plates, geometric nonlinearity.

Berke [1971] proposed an algorithm to satisfy the optimality criteria, considering that if a criterion works for statically determinate structures, then it would converge in a few iterations for most indeterminate structures (in the same manner as the FSD criterion). Berke's work was extended to multiple constraints by Gellatly and Berke [1971; 1973] who proposed the envelope method for multiple displacement constraint structures. Nagtegaal [1973] directly used the displacement constraint equations to formulate an iteration scheme using the Lagrange multiplier. Berke and Khot [1974] proposed an intuitive iteration scheme for Lagrange multipliers. Khot et al. [1979] applied classical optimality criteria method for both stress and displacement constraints. For a more detailed literature survey on optimality criteria methods, the reader is referred to a recent paper by Lógó [2005].

The main focus of the present study is to find the optimum location of the ribs in stiffened panels. Layout optimization problems for rib reinforcement were considered almost two decades ago by Bendsøe and Kikuchi [1988]. An overview of the research in layout and topology optimization is given in the paper by Rozvany et al. [1995]. Stok and Mihelic [1996] presented a method to identify the rib location by performing thickness distribution. Chung and Lee [1997] employed a topology optimization technique to identify the size of the ribs for a predetermined rib layout. Lee et al. [2000] have used modal design sensitivity analysis for topology optimization of an automobile hood. Lam and Santhikumar [2003] developed a method to find the optimum locations of the ribs subject to design constraints using thickness optimization with the uniform strain energy density criterion. All of the above mentioned studies on the stiffened panels are based on linear analysis, whereas many plate and shell structures may display nonlinear behavior under applied loads.

In this study, first an optimality criterion, called uniform average of strain energy variation (UASEV), is developed for thickness optimization in the general case of the combination of membrane and bending deformations. It will be shown that the USED criterion (with strain energy density defined as the strain energy stored in unit volume) cannot be used for thickness optimization, unless the structure is in pure membrane or in pure bending mode. Subsequently, the result of the thickness optimization with the proposed criterion is used for locating the ribs on the original panel. It is shown that the load-carrying capacity of the original panel subject to design constraints may significantly be improved with the same volume of the material. Illustrated applications are also presented.

2. Optimality criterion for thickness optimization

In this section, an optimality criterion is developed for thickness optimization of plates and shells modeled by finite elements. In our study, the thickness of each element in the finite element mesh is considered as a design variable, and an optimization criterion is found subject to constant total volume (Figure 1).

We assume that a plate or shell structure with uniform material properties is modeled by N facet elements. This structure is analyzed under the conservative and proportional nodal force vector λR in which R is a constant reference nodal force vector, and λ is a load level factor which can be gradually increased until a design constraint (displacement, stress, or stability constraint) is violated. At this instant, λR is called the *load capacity* of this structure with respect to design constraints. The optimization problem is to find the optimum thickness t_i $(i = 1, \ldots, N)$ for each element in order to maximize λ subject to constant total volume of the material (that is, $V = V_0$, where V is the total volume of the material.)

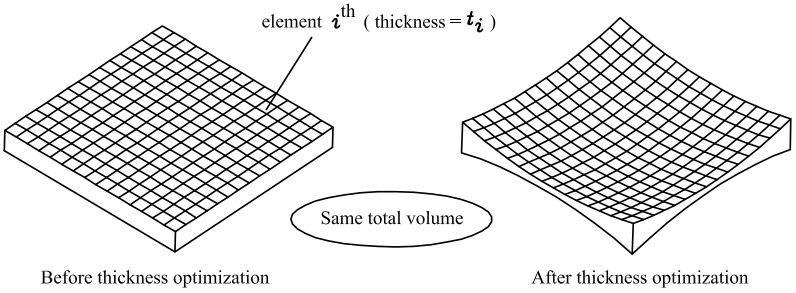

Figure 1. Concept of thickness optimization subject to constant volume.

The Lagrangian for this optimization problem is

$$L = -\lambda + \mu(V - V_0), \tag{1}$$

where μ is the Lagrange multiplier. The Karush–Kuhn–Tucker (KKT) conditions [Arora 1989] for minimization of L with respect to each design variable t_i results in

$$\frac{\partial L}{\partial t_i} = 0; \quad (i = 1, \ldots, N). \tag{2}$$

Thus

$$-\frac{\partial \lambda}{\partial t_i} + \mu \frac{\partial V}{\partial t_i} = 0; \quad (i = 1, \ldots, N) \tag{3}$$

or

$$-\frac{\partial \lambda}{\partial t_i} + \mu A_i = 0; \quad (i = 1, \ldots, N), \tag{4}$$

where A_i is the area of the ith element. Now we write the total potential energy of the structure, assuming that the load is conservative and proportional as

$$\Pi = \sum_{i=1}^{N} e_i - \lambda u^T R, \tag{5}$$

where u and λR are the nodal displacement vector in the global coordinate system and the vector of the applied loads, respectively, and e_i is the strain energy of the ith element. Considering Π_{opt} as the total potential energy associated with the optimum design, the equation $\Pi = \Pi_{opt}$ should also be satisfied for the optimum design. Taking the derivative from both sides of this equation with respect to each design variable t_i (noticing that u and λ are also functions of the design variable t_i) we have

$$\frac{\partial e_i}{\partial t_i} + \sum_{j=1}^{m} \frac{\partial \Pi}{\partial u_j} \frac{\partial u_j}{\partial t_i} + \frac{\partial \Pi}{\partial \lambda} \frac{\partial \lambda}{\partial t_i} = 0; \quad (i = 1, \ldots, N), \tag{6}$$

where m is the number of the nodal displacement components. From the principle of stationary total potential energy we have $\frac{\partial \Pi}{\partial u} = 0$, thus Equation (6) changes to

$$\frac{\partial e_i}{\partial t_i} + 0 - u^T R \frac{\partial \lambda}{\partial t_i} = 0, \tag{7}$$

in which $\frac{\partial \Pi}{\partial \lambda}$ has been substituted by $-u^T R$. Substituting for $\frac{\partial \lambda}{\partial t_i}$ from Equation (7) into Equation (4) results in

$$\frac{-1}{u^T R} \frac{\partial e_i}{\partial t_i} + \mu A_i = 0 \tag{8}$$

or

$$\frac{1}{A_i} \frac{\partial e_i}{\partial t_i} = \mu u^T R. \tag{9}$$

This equation (hereinafter called the uniform average of strain energy variation (UASEV) criterion), states that a design in which the value of $\tilde{e}_i = \frac{1}{A_i} \frac{\partial e_i}{\partial t_i}$ is the same for all elements is a candidate for optimality. It should be noted that since the second variation of the Lagrangian is not examined in this study, this optimality criterion is only an empirical local-optimality condition. Also, since this criterion is satisfied only at the final load (load capacity), it assumes monotonic structural behavior and excludes path dependency.

In the case that the structure is made of an isotropic material with the Poisson's ratio ν and the Young's modulus $E_\circ$, the strain energy of the ith element is computed as

$$e_i = \frac{1}{2} \int_{A_i} \left(\{\varepsilon_m^\circ\}^T D_i^{(1)} \{\varepsilon_m^\circ\} + \{\varepsilon_b^\circ\}^T D_i^{(2)} \{\varepsilon_b^\circ\} \right) dA_i, \tag{10}$$

where $D_i^{(1)}$ and $D_i^{(2)}$ are the membrane and flexural stiffness matrices at the location of the ith element with thickness t_i

$$D_i^{(1)} = \frac{E_\circ t_i}{1-\nu^2} \begin{bmatrix} 1 & \nu & 0 \\ \nu & 1 & 0 \\ 0 & 0 & \frac{1-\nu}{2} \end{bmatrix}, \qquad D_i^{(2)} = \frac{E_\circ t_i^3}{12(1-\nu^2)} \begin{bmatrix} 1 & \nu & 0 \\ \nu & 1 & 0 \\ 0 & 0 & \frac{1-\nu}{2} \end{bmatrix}, \tag{11}$$

and $\{\varepsilon_m^\circ\} = \{\varepsilon_x^\circ \varepsilon_y^\circ \gamma_{xy}^\circ\}^T$ and $\{\varepsilon_b^\circ\} = \{\kappa_x^\circ \kappa_y^\circ \kappa_{xy}^\circ\}^T$ are the membrane and flexural strains in the mid-surface of the ith element, respectively.

Now the average strain energy variation can be described as

$$\tilde{e}_i = \frac{1}{A_i} \frac{\partial e_i}{\partial t_i} = \frac{1}{2A_i} \int_{A_i} \left(\{\varepsilon_m^\circ\}^T \frac{D_i^{(1)}}{t_i} \{\varepsilon_m^\circ\} + \{\varepsilon_b^\circ\}^T \frac{3D_i^{(2)}}{t_i} \{\varepsilon_b^\circ\} \right) dA_i. \tag{12}$$

One can easily see that $\tilde{e}_i$ computed by Equation (12) in the general case of combination of membrane and bending deformations is different from the strain energy density, which is usually defined as $e_i/(t_i A_i)$:

$$\bar{e}_i = \frac{e_i}{t_i A_i} = \frac{1}{2A_i} \int_{A_i} \left(\{\varepsilon_m^\circ\}^T \frac{D_i^{(1)}}{t_i} \{\varepsilon_m^\circ\} + \{\varepsilon_b^\circ\}^T \frac{D_i^{(2)}}{t_i} \{\varepsilon_b^\circ\} \right) dA_i \tag{13}$$

As a result, thickness optimization of plates and shells using a uniform strain energy density criterion with the values computed by Equation (13) in the general case of the combination of membrane and

bending deformations is unjustified. However in case of pure membrane strain energy (that is, $\{\varepsilon_b^\circ\} = 0$), using USED criteria instead of UASEV leads to the same result (because in this case Equations (12) and (13) are equivalent). Also, in the case of the pure bending strain energy (that is, $\{\varepsilon_m^\circ\} = 0$) results are again the same, since based on Equations (12) and (13), uniform distribution of $\bar{e}_i$ and uniform distribution of $\tilde{e}_i$ in the case of $\{\varepsilon_m^\circ\} = 0$ are equivalent by a scale factor of 3.

Considering element thicknesses as the design variables is not the only possible approach in thickness optimization. One may instead consider nodal thicknesses as the design variables, which has the advantage of leading to a smooth thickness profile. However in that case, the related equations are more complicated, since each design variable is connected to more than one element. For example, $\partial V/\partial t_i$ is no longer equal to A_i when passing from Equation (3) to Equation (4) , or $\partial e_i/\partial t_i$ in Equation (6) changes to the summation of the same term for all elements sharing the nodal thickness t_i. In Section 4 it is explained how using the proposed method with linear interpolation can lead to a smooth thickness profile as well.

3. Recurrence relation

In order to satisfy the UASEV criterion, a resizing algorithm has to be employed in the optimization process. First, we rewrite Equation (9) assuming that at the optimum design $\mu u^T R = 1/\Lambda$,

$$\tilde{e}_i = \frac{1}{A_i}\frac{\partial e_i}{\partial t_i} = \frac{1}{\Lambda}. \tag{14}$$

Thus

$$1 = \Lambda \tilde{e}_i. \tag{15}$$

A recurrence relation for resizing the thickness of each element may be written by multiplying both sides of Equation (15) by t_i and taking the rth root as

$$(t_i)_{\upsilon+1} = (t_i)_\upsilon (\Lambda \tilde{e}_i)_\upsilon^{1/r}, \tag{16}$$

where $\upsilon + 1$ and υ are the iteration numbers, and r is the step size parameter which can be changed by assigning appropriate value [Stok and Mihelic 1996; Lam and Santhikumar 2003]. The value of Λ at the optimal design may be found from Equation (15) by minimizing the sum of the squares of the residuals at iteration υ as

$$\mathrm{Res}_\upsilon = \sum_{i=1}^{N} (1 - \Lambda \tilde{e}_i)^2. \tag{17}$$

Thus

$$\frac{d\,\mathrm{Res}_\upsilon}{d\Lambda} = 0 \Rightarrow \Lambda = \Big(\sum_{i=1}^{N} \tilde{e}_i\Big) / \Big(\sum_{i=1}^{N} \tilde{e}_i{}^2\Big). \tag{18}$$

Substituting Equation (18) into Equation (16) we finally obtain the recurrence relation

$$(t_i)_{\upsilon+1} = (t_i)_\upsilon \left(\Big(\sum_{i=1}^{N} \tilde{e}_i\Big) / \Big(\sum_{i=1}^{N} \tilde{e}_i{}^2\Big) \tilde{e}_i \right)_\upsilon^{1/r}, \tag{19}$$

which is used to optimize the thickness of each element iteratively. In order to keep the total volume equal to constant V_0, after each iteration, all t_i are scaled by a scale factor β:

$$\beta = \frac{V_0}{V} = \frac{V_0}{\sum_{i=1}^{N} t_i A_i}. \tag{20}$$

The iterative process of thickness optimization may be stopped when the following condition is satisfied:

$$\Delta(\lambda R)_\upsilon \leq (\text{tol})\Delta(\lambda R)_1, \tag{21}$$

where $\Delta(\lambda R)_1$ and $\Delta(\lambda R)_\upsilon$ are the changes in the load capacity of the structure in the first and υth iterations respectively, and tol is usually chosen in the range of tol $\leq 10^{-2}$, depending on the accuracy required.

4. Methodology

After performing the thickness optimization, the optimal shape is still rough and should be smoothed by passing to nodal thicknesses. The thickness of the plate at each node is found by taking the average of the thicknesses of all elements connected to that node. Then, a smooth thickness profile may be created by linear interpolation using nodal thicknesses. Finally the regions where elements have higher thickness values are identified as potential rib locations.

In the next step, stiffeners with variable height according to the results found in the first step are added to the plate with constant thickness. The height of the ribs varies proportionally to the obtained thickness distribution, but not more than a maximum value considered in the design constraint. Finally, thicknesses of the plate and stiffeners are found such that the constant volume constraint is satisfied. The whole process may be repeated to find additional stiffeners.

As an example, Figure 2 shows how the potential locations for adding the stiffeners are found for a simple plate. Variation of the thickness after performing the thickness optimization is shown by thickness contours. Considering the cross sections of the plate at different locations, one can identify the locations of the local maximum thickness at each section. The lines which connect these points of local maximum thickness are called the lines of maximum thickness, and are selected as the potential locations for stiffeners. Any design constraint or limitation is also considered in locating the stiffeners. The locations and the directions of the sections are arbitrary, and usually they are selected by the designer in a way to perform the design with the least number of sections. Obviously, the final design may not be completely unique, and will somehow depend on the designer's point of view.

This method is similar to the one used by Stok and Mihelic [1996] and Lam and Santhikumar [2003], except that in their studies, the USED criterion was used instead of UASEV. As mentioned before, it is important to note that in the general case of the combination of membrane and bending deformations, using the USED criterion instead of UASEV is unjustified, and only in the case of pure membrane or pure bending behavior are the results the same.

In topology optimization a checkerboard pattern, which is an unnatural result with artificially high stiffness, may frequently occur [Díaz and Sigmund 1995; Jog and Haber 1996]. Several techniques have been proposed to avoid such a checkerboard pattern as an optimal solution [Poulsen 2002; Sigmund and Petersson 1998; Zhou et al. 2001]. In this study we use a simple procedure similar to the one used

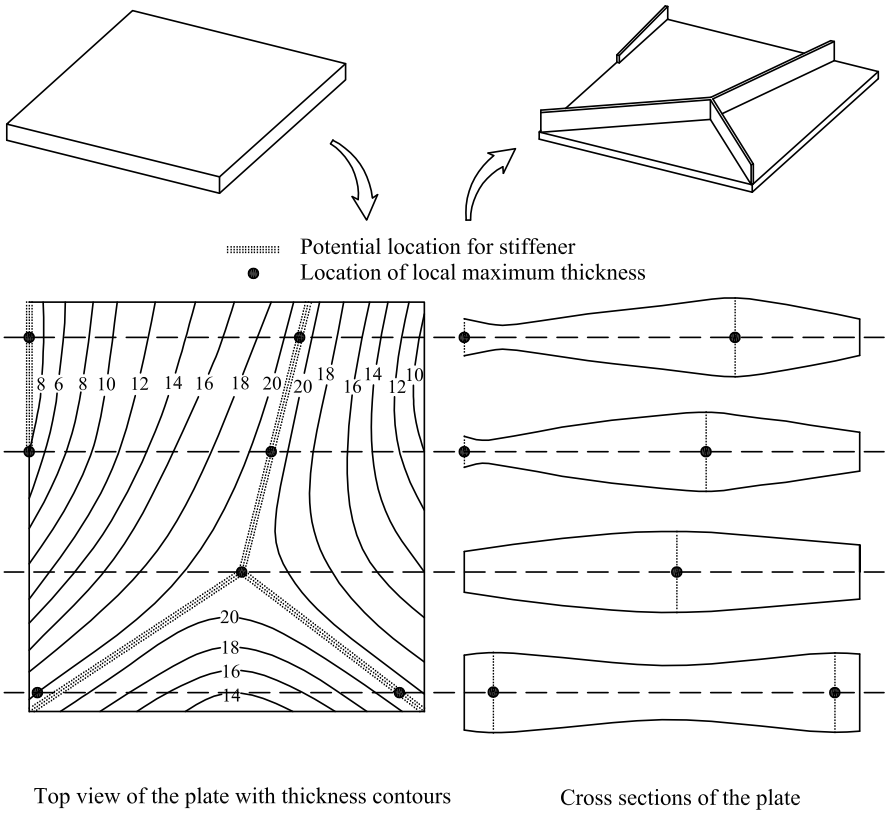

Figure 2. Identifying potential locations for stiffeners using thickness optimization.

by Gáspár et al. [2001], in which a primary meshing is subdivided into further finite elements called secondary elements. In this study, first a primary mesh is considered with square elements, and then each square in the primary mesh is divided into two triangular elements. The new thickness of each square in the primary mesh (after each iteration) is found by taking the average of the new thicknesses of its two triangular elements.

Strain energy for most of the elements available in literature is not accurate when used in coarse meshes [Felippa 2003]. This makes the problem of thickness optimization very expensive, since a large number of elements is needed in nonlinear analysis to get a desirable accuracy. On the other hand, when modeling the ribs in stiffened plates (after performing the thickness optimization and selecting the potential places to add the ribs), it frequently happens that some elements have very high or very low geometrical aspect ratios in the stiffener parts. Response of these elements can affect the response of the whole structure, leading to erroneous results about the behavior of the stiffened plate [Felippa 2003]. Thus, it is preferable to model the structure with an element which has the least aspect ratio sensitivity and highest accuracy for strain energy.

The element in this study is a facet triangular shell element with 3 nodes and 6 degrees of freedom per node (3 translations and 3 rotations) [Khosravi et al. 2007]. This element is a combination of the discrete Kirchhoff triangular plate bending element (DKT) [Batoz et al. 1980], and the optimal triangular

membrane element (OPT) [Felippa 2003]. The OPT membrane element has been formulated based on the ANDES (assumed natural deviatoric strain) template, and for any arbitrary aspect ratio its strain energy is accurate. In a recent paper [Khosravi et al. 2007], it has been shown that using this element leads to acceptable results even in case of relatively coarse meshes. As a result, the cost of the optimization in a nonlinear regime may be extensively reduced using this element.

In this study, a corotational approach is used to analyze the structure with geometric nonlinearity. In this approach the contribution of the rigid body motion to the total deformation of the element is removed before performing the element computations. This enables one to upgrade the structural elements so as to treat problems with large rotations but small strains. For a detailed explanation of the shell element used in this study and the corotational nonlinear analysis using triangular facet elements, the reader is referred to [Khosravi et al. 2007]. In order to follow the nonlinear load deflection path, the arc length method [Crisfield 1981] is used.

It should be mentioned that recently some doubts have been raised about the mathematical convergence of facet elements [Chapelle and Bathe 2003]. In particular, when refining the mesh, finite element solutions are expected to converge to the exact solution of a well-defined mathematical model. However, some numerical experiments have shown that facet shell elements may not exactly converge when the mesh is refined, although their results lie within a few percent of the reference values [Chapelle and Bathe 2003]. It is believed that the best shell elements are formulated using 3D continuum mechanics incorporating shell theory assumptions. However facet elements are used in this study since the formulation of a corotational approach using curved elements is extremely difficult to perform and is not even well developed.

5. Numerical results

In this section, four examples are presented. In the first and second examples, the proposed UASEV criterion is used for thickness optimization of plate structures, and results are compared with those found by using the USED criterion, that is, Equation (13) instead of Equation (12). The third and fourth examples show the application of thickness optimization in stiffener location and load capacity maximization of plates subject to constant volume. In all examples, Equations (19)–(21) with $\text{tol} = 10^{-2}$ are used for thickness optimization.

Example 1. Figure 3 shows a cantilever plate subject to the shear load F and axial force $P = 20\,F$ at the tip. The dimensions of the plate are $40\,\text{cm} \times 4\,\text{cm}$ with overall thickness $t = 0.4\,\text{cm}$, and the plate is made of isotropic material (steel) with the following mechanical properties: $E = 200\,\text{GPa}$, $G = 77\,\text{GPa}$, $\nu = 0.3$.

The objective is to perform the thickness optimization in order to maximize the load capacity F subject to constant volume. It is assumed that the load capacity F is found based on the displacement $W = 1\,\text{cm}$, where W is the vertical deflection at the tip of the plate. The plate is modeled by 40 triangular elements, and due to symmetry, only half of the plate is analyzed.

Nonlinear analysis results in $F = 49.81\,\text{N}$ as the initial load capacity of the plate. Figure 4 shows the results of thickness optimization subject to constant volume, using UASEV and also USED criteria. In both cases, convergence is achieved in 5 iterations, with $r = 2$ as the step size parameter. Nonlinear behavior of the plate optimized by UASEV and USED criteria is also shown in Figure 5.

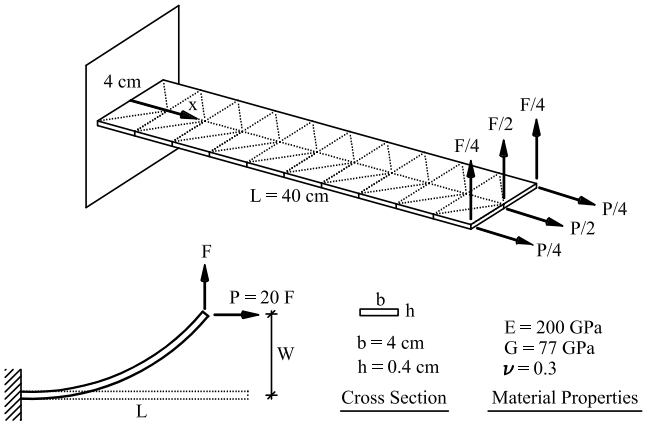

Figure 3. Cantilever plate subject to axial and shear forces at the tip.

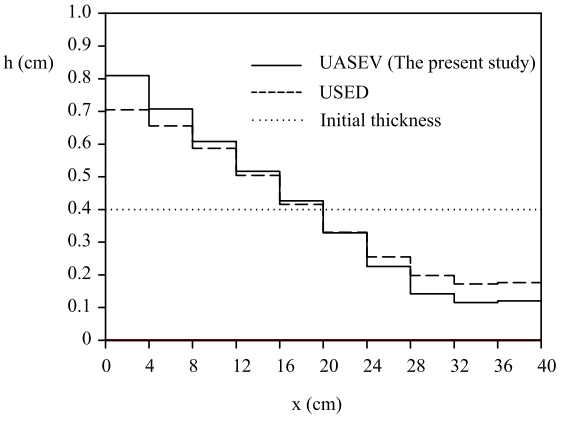

Figure 4. Variation of the thickness over the length of the cantilever plate after optimization.

It is observed that optimization using the UASEV criterion increases the load capacity of the plate to $F = 150.36\,N$, compared to $F = 131.16\,\text{N}$ obtained by using USED criterion. In Figure 5, it is interesting to note that in the range of $W \leq 0.75\,\text{cm}$, the load capacity of the plate optimized by UASEV criterion is slightly less than that of the one optimized by USED; however since the optimality criteria are applied at the limit point (that is, $W = 1\,\text{cm}$), UASEV finally overcomes USED and leads to a higher load capacity.

Example 2. Figure 6 shows a simply supported square plate under the biaxial compressive edge forces $N_x = N_y$. The dimensions of the plate are $80\,\text{cm} \times 80\,\text{cm}$ with overall thickness $t = 0.4\,\text{cm}$, and the plate is made of isotropic material (steel) with the following mechanical properties: $E = 200\,\text{GPa}$, $G = 77\,\text{GPa}$, $\nu = 0.3$.

In order to initiate the lateral deflection, an imperfection in the form of a half sine wave with the maximum value 1 mm at the center of the plate is considered. The objective is to optimize the thickness of the plate, while having the same total volume, in order to maximize the load capacity for $W = 0.4\,\text{cm}$, where W is the vertical deflection at the center of the plate. The plate is modeled by 800 triangular

elements, and due to symmetry only a quarter of the plate is analyzed. Performing the nonlinear analysis results in $N_x = N_y = 369.5$ N/cm as the initial load capacity of this plate.

Figures 7a and 7b show the results of thickness optimization subject to constant volume for a quarter of the plate using Equations (19)–(21) in 8 iterations, and UASEV and USED criteria, respectively. In both cases $r = 4$ has been considered as the step size parameter. It is observed that optimization based on USED criteria tends to reduce the thickness in the middle of the plate, and to increase it on the corners and mid-sides. Instead, UASEV criterion tends to reduce the thickness on the mid-sides and to increase it on the corners and somewhat in the middle. Figure 8 shows the change of load-carrying capacity of the plate during the thickness optimization. Nonlinear analysis of an optimal plate under the applied loads shows that the load capacity of this plate has been increased to $N_x = N_y = 584.3$ N/cm, and $N_x = N_y = 509.2$ N/cm for UASEV and USED criteria, respectively, while having the same total

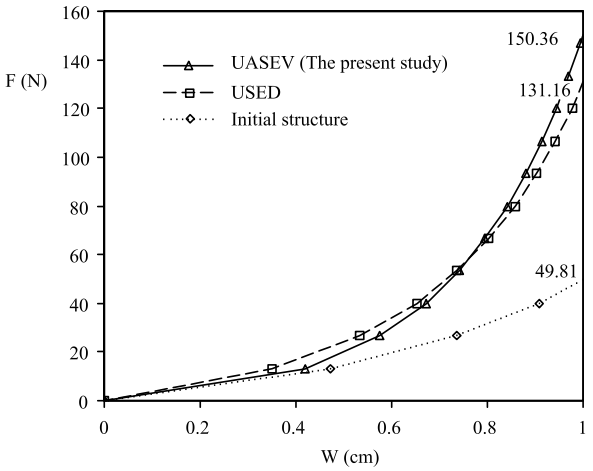

Figure 5. Nonlinear behavior of the cantilever plate before and after optimization.

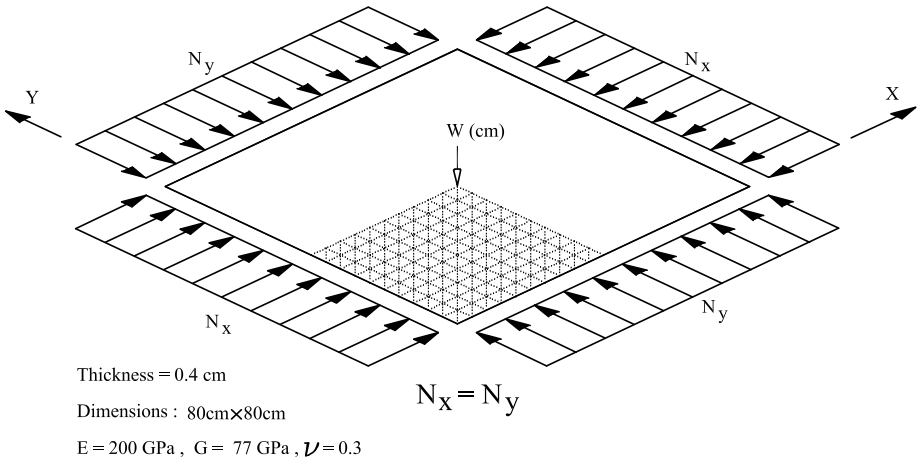

Figure 6. Square plate with simple supports subjected to biaxial compressive forces.

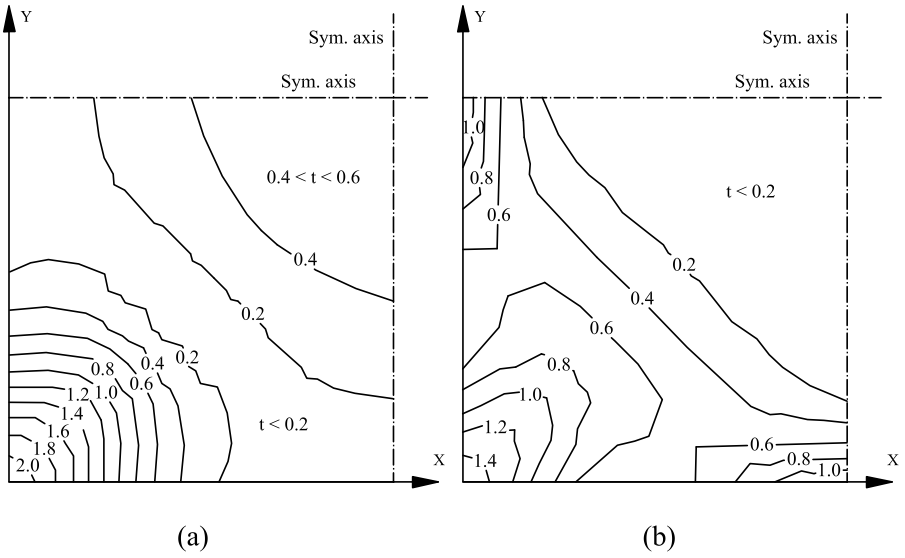

Figure 7. Results of thickness optimization (cm) for a quarter of the plate shown in Figure 6: (a) UASEV criterion; (b) USED criterion.

volume. Although using any one of these two criteria increases the strength (or load capacity) of the plate, it is obvious that the UASEV criterion is more efficient than that of USED.

Example 3. In this example the application of the UASEV criterion is shown for thickness optimization, and subsequently stiffener location in a stiffened plate. Figure 9 shows an 80×80 cm simply-supported square plate with overall thickness $t = 0.4$ cm and a 24 cm $\times$ 24 cm square hole in the center. Loading and material properties are similar to those in the previous example. Also, an imperfection in the form of a half sine wave with the value of 1 mm around the central hole is considered to initiate the lateral deflection. The objective is to optimize the thickness and find the potential stiffener locations subject to constant volume, in order to maximize the load capacity for $W = 0.4$ cm, where W is the deflection at

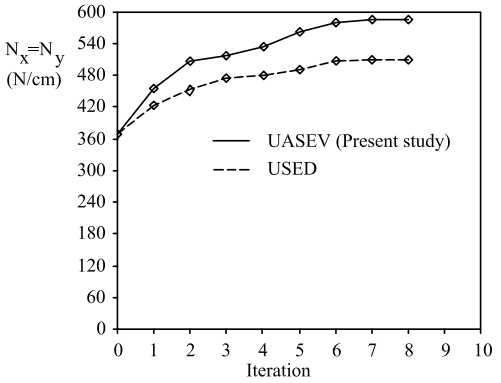

Figure 8. Change of load-carrying capacity of the plate shown in Figure 6 during the thickness optimization using USED and UASEV criteria.

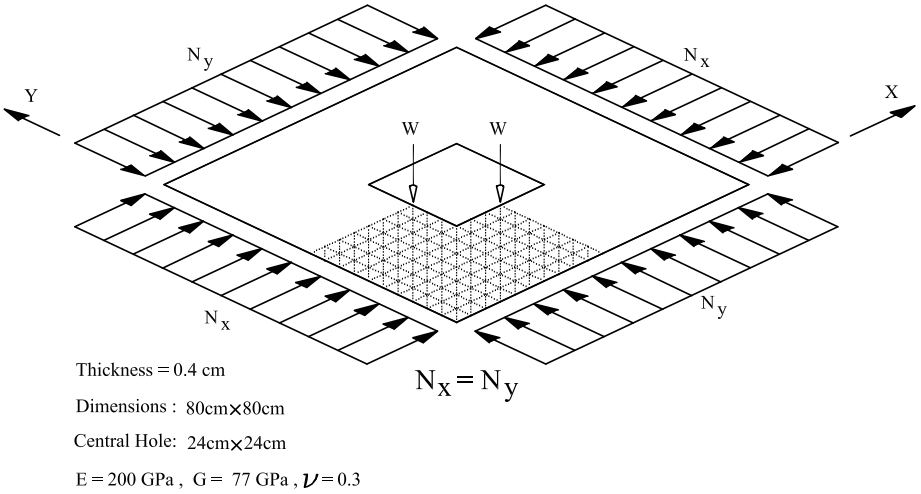

Figure 9. Square plate with a square hole in the center and simple supports, subjected to biaxial compressive forces.

the midpoint of the hole edges. In this example, the following design constraints should also be satisfied for the final design:

- The maximum height of the stiffeners is 5 cm.
- The stiffeners and the plate have the same thickness in the final design.

Similar to the previous example, a quarter of the plate is modeled by 182 triangular elements. Performing the nonlinear analysis results in $N_x = N_y = 290.8\,\mathrm{N/cm}$ as the load capacity of this plate for $W = 0.4\,\mathrm{cm}$. Thickness optimization is performed using the UASEV criterion with $r = 4$ as the step size parameter. The iterative process converged after 9 iterations. Variation of the thickness for a quarter of the plate, based on the results of thickness optimization subject to constant total volume is shown in Figure 10. Load carrying capacity of this plate after performing the thickness optimization, has increased to $N_x = N_y = 654.3\,\mathrm{N/cm}$.

Based on this shape, and predefined design constraints mentioned above, stiffeners are located on the lines of maximum thicknesses (as shown in Figure 11) on a plate with constant thickness. Height of the stiffeners are proportional to the thickness of the elements, with the maximum value of 5 cm according to the first design constraint. Keeping the total volume equal to the initial volume $2329.6\,\mathrm{cm}^3$, and considering the same thickness for stiffeners and plate (per the second design constraint) a new overall thickness of $t = 0.36\,\mathrm{cm}$ is found for the plate and the stiffeners. A nonlinear analysis of this stiffened plate shows that the load capacity has increased to $N_x = N_y = 560.4\,\mathrm{N/cm}$ compared to $N_x = N_y = 290.8\,\mathrm{N/cm}$ for the initial plate, however it has been reduced compared to $N_x = N_y = 654.3\,\mathrm{N/cm}$ for the plate with optimized thickness.

Example 4. A plate similar to the one in Example 3 is considered under the downward surface load q. Boundary conditions are similar to those in Example 3 except that in-plane deflections are not allowed for all four edges. As a result, membrane forces arise during the deflections due to bending. The objective is

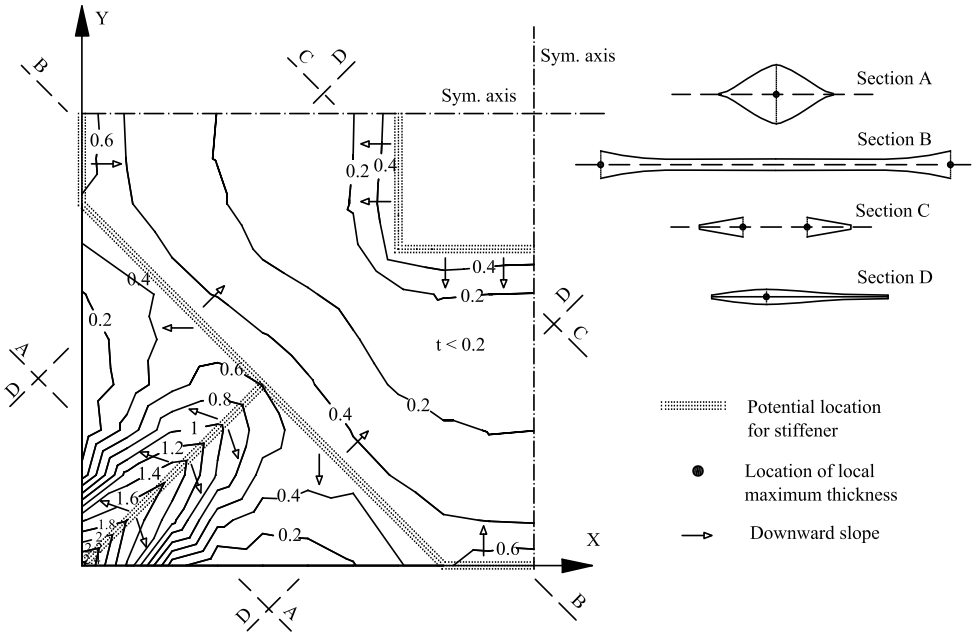

Figure 10. Result of thickness optimization (cm) for a quarter of the plate shown in Figure 9. Thicknesses of the sections have been exaggerated for better view.

to maximize the load capacity for $W = 0.3$ cm using UASEV criterion, subject to constant total volume. The following design constraints should also be satisfied in this problem:

- The maximum height of the stiffeners is 10 cm.
- The thickness of the stiffeners is 0.4 cm.

A quarter of the plate is modeled by 182 triangular elements. Also, we can see that a nonlinear analysis results in $q = 0.318\,\mathrm{N/cm^2}$ as the load capacity of this plate. In the next step, UASEV criterion with $r = 4$ is employed for thickness optimization. The new thickness distribution and potential locations for stiffeners are shown in Figure 12, and are found after 9 iterations. The load-carrying capacity of this plate after performing the thickness optimization has increased to $q = 0.865\,\mathrm{N/cm^2}$.

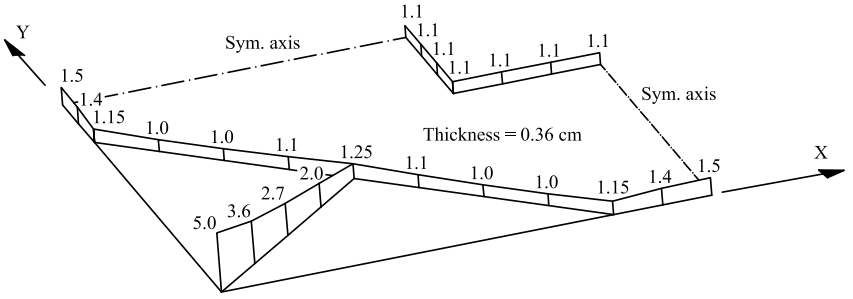

Figure 11. A quarter of the plate shown in Figure 9 (Example 3) with stiffeners at potential locations. Numbers show the height of the stiffeners (cm).

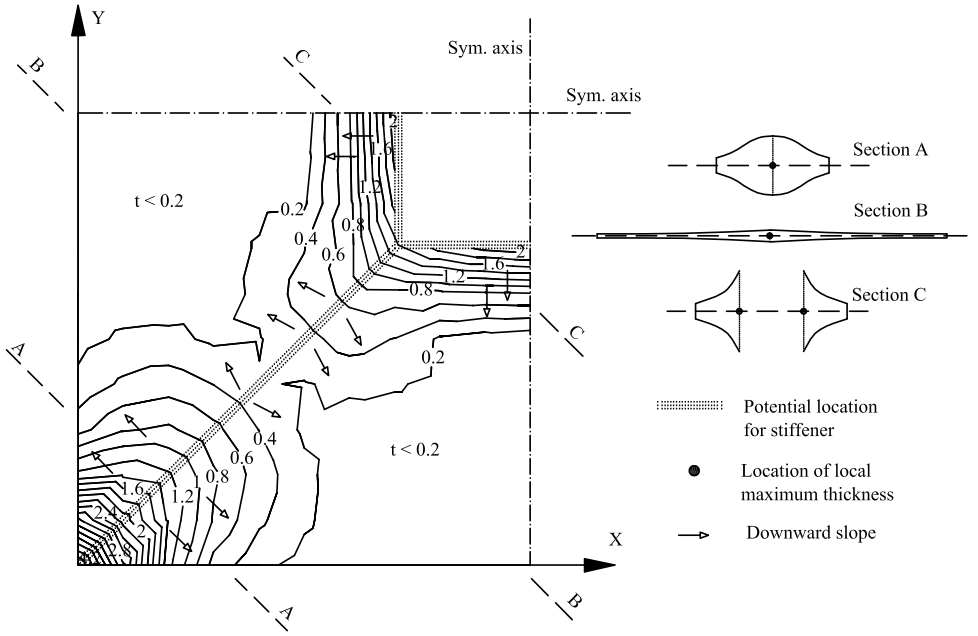

Figure 12. Result of thickness optimization (cm) for a quarter of the plate shown in Figure 9 with hinged supports ($u = v = w = 0$ at the edges) under the downward surface pressure load. Thicknesses of the sections have been exaggerated for a better view.

Figure 13 shows the stiffeners located on the lines of maximum thickness, with their height proportional to the new thickness of the elements, but not more than 10 cm, and their thickness equal to 0.4 cm according to the design constraint. Keeping the total volume equal to the initial volume, a new thickness $t = 0.339 \approx 0.34$ cm is found for the plate. Nonlinear analysis shows that the load capacity for $W = 0.3$ cm has increased to $q = 1.26\,\mathrm{N/cm^2}$ compared to $q = 0.318\,\mathrm{N/cm^2}$ for the initial plate, and compared to $q = 0.865\,\mathrm{N/cm^2}$ for the plate with optimized thickness.

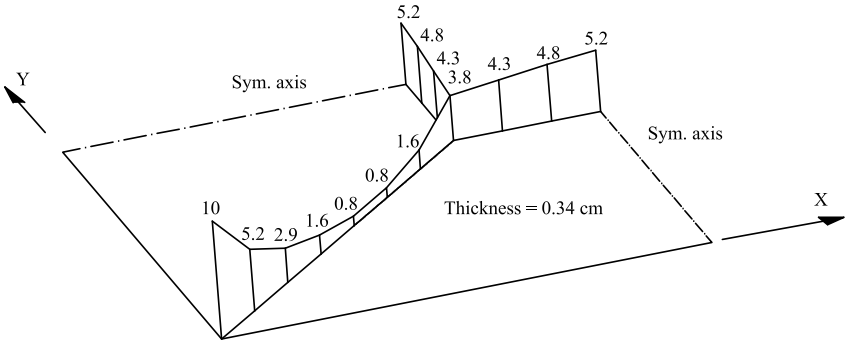

Figure 13. A quarter of the plate in Example 4 with stiffeners at potential locations. Numbers show the height of the stiffeners (cm).

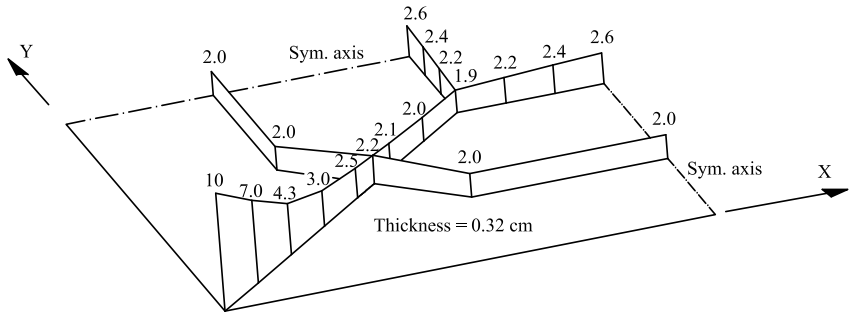

Figure 14. A quarter of the plate in Example 4 with stiffeners at potential locations after two rounds of optimization. Numbers show the height of the stiffeners (cm).

It should be mentioned that once the ribs are placed on a plate, structural behavior of the plate changes considerably. Thus, as mentioned before, it seems appropriate to repeat the optimization process for the stiffened plate, to obtain any further possible stiffener locations, and also modify the heights of the previously located stiffeners. Figure 14 shows the result of the optimized plate in Example 4 after the second round of optimization. It may be seen that a new series of stiffeners are found and the heights of the previous stiffeners have also been modified. Performing nonlinear analysis, the load capacity of the stiffened plate after the second round of optimization is found to be $q = 1.57\,\mathrm{N/cm^2}$ compared to $q = 1.26\,\mathrm{N/cm^2}$ after the first round.

6. Conclusion

In this study a methodology for rib location and design optimization of stiffened plates based on an optimality criterion for thickness optimization is presented. The optimality criterion for thickness optimization (called UASEV in this study) states that in an optimum design, the derivative of the strain energy with respect to the thickness, over the area of element, is the same for all elements. It was shown that in the general case of the combination of membrane and bending deformations, using the USED criterion instead of UASEV is unjustified. Only in case of pure membrane or pure bending behavior are their results the same. Applying the proposed criterion through an iterative process, it is possible to find the potential locations to add stiffeners and increase the strength of the plate while consuming the same amount of material.

References

[Arora 1989] J. S. Arora, *Introduction to optimum design*, McGraw-Hill, New York, 1989.

[Batoz et al. 1980] J. L. Batoz, K. J. Bathe, and L. W. Ho, "A study of three-node triangular plate bending elements", *Int. J. Numer. Methods Eng.* **15**:12 (1980), 1771–1812.

[Bendsøe 1989] M. P. Bendsøe, "Optimal shape design as a material distribution problem", *Struct. Multidiscip. O.* **1**:4 (1989), 193–202.

[Bendsøe and Kikuchi 1988] M. P. Bendsøe and N. Kikuchi, "Generating optimal topologies in structural design using a homogenization method", *Comput. Methods Appl. Mech. Eng.* **71**:2 (1988), 197–224.

[Bendsøe and Mota Soares 1993] M. P. Bendsøe and C. A. Mota Soares, "Topology design of structures", pp. xvi+569 in *Proceedings of the NATO Advanced Research Workshop held in Sesimbra, June 20–26, 1992* (Sesimbra, Portugal), edited by

M. P. Bendsøe and C. A. M. Soares, NATO Advanced Science Institutes Series E: Applied Sciences **227**, Kluwer, Dordrecht, 1993.

[Bendsøe and Sigmund 1999] M. P. Bendsøe and O. Sigmund, "Material interpolation schemes in topology optimization", *Arch. Appl. Mech.* **69**:9-10 (1999), 635–654.

[Bendsøe and Sigmund 2003] M. P. Bendsøe and O. Sigmund, *Topology optimization: theory, methods and applications*, Springer, Berlin, 2003.

[Berke 1971] L. Berke, "An efficient approach to the minimum weight design of deflection limited design", technical report AFFDL-TR-70-4-FDTR, Air Force Flight Dynamics Laboratory, 1971.

[Berke and Khot 1974] L. Berke and N. S. Khot, "Use of optimality criteria methods for large scale systems", *AGARD Lect. Ser.* **70** (1974), 1–29.

[Chapelle and Bathe 2003] D. Chapelle and K. J. Bathe, *The finite element analysis of shells—fundamentals*, Computational fluid and solid mechanics, Springer, Berlin, 2003.

[Chung and Lee 1997] J. Chung and K. Lee, "Optimal design of rib structures using the topology optimization technique", *Proc. Inst. Mech. Eng. C J. Mech. Eng. Sci.* **211**:6 (1997), 425–437.

[Crisfield 1981] M. A. Crisfield, "A fast incremental-iterative solution procedure that handles 'snap-through'", *Comput. Struct.* **13**:1-3 (1981), 55–62.

[Díaz and Sigmund 1995] A. R. Díaz and O. Sigmund, "Checkerboard patterns in layout optimization", *Struct. Multidiscip. O.* **10**:1 (1995), 40–45.

[Felippa 2003] C. A. Felippa, "A study of optimal membrane triangles with drilling freedoms", *Comput. Methods Appl. Mech. Eng.* **192**:16-18 (2003), 2125–2168.

[Gallagher 1973] R. H. Gallagher, "Fully stressed design", pp. 19–32 in *Optimum structural design: theory and applications*, edited by R. H. Gallagher and O. C. Zienkiewicz, Wiley, London, 1973.

[Gáspár et al. 2001] Z. S. Gáspár, J. Lógó, and G. I. N. Rozvany, "On design-dependent constraints and singular topologies", *Struct. Multidiscip. O.* **21**:2 (2001), 164–172. Addenda in **24**:2 (2002), 338–342.

[Gellatly and Berke 1971] R. A. Gellatly and L. Berke, "Optimal structural design", technical report, Air Force Flight Dynamics Laboratory, 1971. AFFDL-TR-70-165.

[Gellatly and Berke 1973] R. A. Gellatly and L. Berke, "Optimality criterion based algorithms", pp. 33–49 in *Optimum structural design: theory and applications*, edited by R. H. Gallagher and O. C. Zienkiewicz, Wiley, London, 1973.

[Jog and Haber 1996] C. S. Jog and R. B. Haber, "Stability of finite element models for distributed-parameter optimization and topology design", *Comput. Methods Appl. Mech. Eng.* **130**:3-4 (1996), 203–226.

[Khosravi et al. 2007] P. Khosravi, R. Ganesan, and R. Sedaghati, "Corotational nonlinear analysis of thin plates and shells using a new shell element", *Int. J. Numer. Methods Eng.* **69**:4 (2007), 859–885.

[Khot et al. 1979] N. S. Khot, L. Berke, and V. B. Venkayya, "Comparison of optimality criteria algorithms for minimum weight design of structures", *AIAA J.* **17**:2 (1979), 182–190.

[Lam and Santhikumar 2003] Y. C. Lam and S. Santhikumar, "Automated rib location and optimization for plate structures", *Struct. Multidiscip. O.* **25**:1 (2003), 35–45.

[Lee et al. 2000] T. H. Lee, S. Y. Han, and J. K. Lim, "Topology optimization of the inner reinforcement for an automobile hood using modal design sensitivity analysis", *Key Eng. Mater.* **183–187** (2000), 439–444.

[Lógó 2005] J. Lógó, "New type of optimal topologies by iterative method", *Mech. Based Des. Struct. Mach.* **33**:2 (2005), 149–171.

[Lógó and Ghaemi 2002] J. Lógó and M. Ghaemi, "Topology optimization by SIMP method", in *Proceedings of the 9th International Conference on Numerical Methods and Computational Mechanics* (Miskolc, Hungary), edited by A. Galántay and G. Szeidl, 2002.

[Maute et al. 1998] K. Maute, S. Schwarz, and E. Ramm, "Adaptive topology optimization of elastoplastic structures", *Struct. Multidiscip. O.* **15**:2 (1998), 81–91.

[Nagtegaal 1973] J. C. Nagtegaal, "A new approach to optimal design of elastic structures", *Comput. Methods Appl. Mech. Eng.* **2**:3 (1973), 255–264.

[Poulsen 2002] T. A. Poulsen, "A simple scheme to prevent checkerboard patterns and one node connected hinges in topology optimization", *Struct. Multidiscip. O.* **24**:5 (2002), 396–399.

[Prager and Taylor 1968] W. Prager and J. E. Taylor, "Problems of optimal structural design", *J. Appl. Mech.* (*Trans. ASME*) **35** (1968), 102–106.

[Rozvany 1997] G. I. N. Rozvany, "Aims, scope, basic concepts and methods of topology optimization", pp. 1–55 in *Topology optimization in structural mechanics*, CISM Courses and Lectures **374**, Springer, Vienna, 1997.

[Rozvany et al. 1995] G. I. N. Rozvany, M. P. Bendsøe, and U. Kirsch, "Layout optimization of structures", *Appl. Mech. Rev.* **48** (1995), 41–111.

[Sigmund and Petersson 1998] O. Sigmund and J. Petersson, "Numerical instabilities in topology optimization—a survey on procedures dealing with checkerboards, mesh-dependencies and local minima", *Struct. Multidiscip. O.* **16**:1 (1998), 68–75.

[Stok and Mihelic 1996] B. Stok and A. Mihelic, "Two-stage design optimization of shell structures", *Struct. Eng. Rev.* **8**:2-3 (1996), 91–97.

[Venkayya 1971] V. B. Venkayya, "Design of optimum structures", *Comput. Struct.* **1**:1-2 (1971), 265–309.

[Venkayya et al. 1968] V. B. Venkayya, N. S. Khot, and V. S. Reddy, "Optimization of structures based on the study of energy distribution", technical report AFFDL-TR-68-150, Air Force Flight Dynamics Laboratory, 1968, Available at http://handle.dtic.mil/100.2/ADA447802.

[Venkayya et al. 1969] V. B. Venkayya, N. S. Khot, and V. S. Reddy, "Energy distribution in an optimum structural design", technical report AFFDL-TR-68-156, Air Force Flight Dynamics Laboratory, 1969.

[Zhou et al. 2001] M. Zhou, Y. K. Shyy, and H. L. Thomas, "Checkerboard and minimum member size control in topology optimization", *Struct. Multidiscip. O.* **21**:2 (2001), 152–158.

Received 7 Sep 2006. Accepted 15 Feb 2007.

PEYMAN KHOSRAVI: peyma_kh@encs.concordia.ca
Department of Mechanical and Industrial Engineering, Concordia University, Montreal, Quebec H3G 1M8, Canada

RAMIN SEDAGHATI: sedagha@encs.concordia.ca
Department of Mechanical and Industrial Engineering, Concordia University, Montreal, Quebec H3G 1M8, Canada

RAJAMOHAN GANESAN: ganesan@vax2.concordia.ca
Department of Mechanical and Industrial Engineering, Concordia University, Montreal, Quebec H3G 1M8, Canada